JOURNAL OF CATALYSIS **176,** 115–124 (1998)
ARTICLE NO. CA981988

Kinetics of CH_4 Decomposition on Supported Cobalt Catalysts

J. Soltan Mohammad Zadeh and Kevin J. Smith[1]

Department of Chemical Engineering, University of British Columbia, 2216 Main Mall, Vancouver, BC, Canada V6T 1Z4

Received August 12, 1997; revised November 21, 1997; accepted November 24, 1997

A model of the kinetics of CH_4 decomposition on supported Co catalysts, at conditions relevant to the two-step CH_4 homologation reaction (450°C, 101 kPa), is presented. The model includes the decomposition of gas phase CH_4 on a Co site and migration of the resulting CH_x fragment from the Co to the support as the key kinetic steps in the decomposition reaction. The migration step is essential to explain the observed kinetics at long reaction times (2–7 min) or high CH_4 feed concentrations (5% CH_4 in Ar). At these conditions, CH_4 decomposition continues at a low but constant rate despite a nominal Co coverage by $CH_x > 1$. The magnitudes of the estimated rate constants for the decomposition and migration steps are used to interpret the observed effects of temperature, catalyst metal loading, support, and K promoter on the CH_4 decomposition kinetics.

INTRODUCTION

In the two-step homologation of CH_4 to higher hydrocarbons (1–4) CH_4 is first decomposed on a suitable catalyst at high temperature and low H_2 partial pressure, generating surface carbonaceous species that are usually referred to as CH_x with $x = 0, 1, 2,$ or 3. These species are subsequently hydrogenated in the second step at low temperature and high H_2 partial pressure to produce higher hydrocarbons such as ethane and propane, herein referred to collectively as C_{2+} products. Unlike CH_4 oxidative coupling or partial oxidation (5–8), the two-step homologation does not produce CO or CO_2 since there is no O_2 in the system. The different temperatures and H_2 partial pressures of the two steps are necessary to overcome the positive Gibbs free energy change associated with the single-step CH_4 homologation reaction: $2CH_4 \rightarrow C_2H_6 + H_2$ (1).

In previous studies of the two-step homologation reaction, CH_4 decomposition was performed over supported group VIII metal catalysts either at high temperature (>300°C) in a dilute stream of CH_4 (1, 9), or with short pulses of CH_4 introduced to the feed gas (10), or at temperatures below 300°C (3). In each case, the moles of CH_4 converted was less than the moles of surface metal atoms available on the catalyst, suggesting less than a monolayer coverage of the metal by the resulting CH_x species. A consequence of the low metal coverage was a low C_{2+} mole yield in the subsequent hydrogenation step since the moles of carbonaceous species available for hydrogenation was limited (1).

One possible approach to increasing the concentration of carbonaceous species on the surface is to react more CH_4 during the activation step by, for example, operating with a higher concentration of CH_4 in the feed. However, under these conditions, the metal sites will likely be rapidly covered by adsorbed CH_x, resulting in a loss in active sites for CH_4 decomposition. Hence, as the metal coverage increases, the number of moles of CH_4 decomposed per unit time would be expected to decrease and eventually reach zero. Previous studies have shown, however, that CH_4 decomposition continues beyond the amount corresponding to a monolayer coverage of the metal sites by CH_x (11). Furthermore, the support is known to influence the number of moles of CH_4 decomposed on the catalyst (12, 13). These observations have been explained by assuming a migration of the carbonaceous species from the metal to the support (12, 14). Spectroscopic evidence for the migration (or spillover) of methyl species generated from methyl halides was reported recently for a Cu metal catalyst supported on SiO_2 (15).

It is well known that the decomposition of CH_4 on metal surfaces yields three different types of carbonaceous species that can be identified by their different reactivities during temperature-programmed surface reaction (TPSR) in H_2 (1, 2, 4, 9, 10, 12, 14). As these species age and as the metal coverage increases, the most reactive carbonaceous species are converted into less reactive forms that, upon hydrogenation, do not produce the desired C_{2+} hydrocarbons (1). Hence, although changing the operating conditions of the first step of the homologation sequence may increase the moles of the carbonaceous species deposited on the catalyst, the type and reactivity of the carbonaceous species are critical since the deposit must be selectively reacted in the subsequent low-temperature hydrogenation step.

The present study focuses on CH_4 decomposition in the first step of the two-step homologation cycle, using relatively high concentrations of CH_4. The effect of increased

[1] To whom correspondence should be addressed. Tel.: (604) 822 3601. Fax: (604) 822 6003. E-mail: kjs@unixg.ubc.ca.

0021-9517/98 $25.00

metal coverage by CH_x is examined, as are the effects of support and promoter. The approach taken in the present study was to develop a model of the CH_4 decomposition kinetics and interpret the effects of different catalyst and operating variables in terms of this model. In this way, the interacting effects of reaction time, temperature, and catalyst can be readily evaluated. The kinetic model includes migration of surface carbonaceous species from the metal to the support. A subsequent submission will describe the hydrogenation of the resulting carbonaceous species and the yield of higher hydrocarbons.

EXPERIMENTAL

1. *Catalyst Preparation*

The cobalt catalysts were prepared by incipient wetness impregnation of the support using an aqueous solution of $Co(NO_3)_2 \cdot 6H_2O$ (+98%, Aldrich). For catalyst series A, silica gel (grade 62, Aldrich) with a BET surface area of 300 m^2/g and pore volume of 1.15 mL/g was used as the support following calcination in air at 500°C for 25 h. After impregnation, the catalysts were dried under vacuum for 37 h at 110°C and then calcined for 10 min at 450°C. Series B catalysts reported in Table 2 were prepared similarly except that there was no high-temperature calcination step and the drying time was extended to at least 10 days. The catalysts were reduced using the temperature-programmed reduction procedure described below. Similar preparation procedures using extended drying times and short calcination times have been shown to provide improved Co dispersions on SiO_2 supports (16).

The preparation method for the series C Co catalysts supported on SiO_2 and Al_2O_3 with and without K promoter, has been reported previously (17).

2. *Reactor and Analytical Setup*

A block flow diagram of the reactor and the on-line analytical equipment used in the present study is shown in Fig. 1. The reactor feed gas flow rate was controlled by Brooks 5878 mass flow controllers and the flow selector valve was used to introduce different gas mixtures to the reactor feed. The fixed-bed microreactor was made from quartz glass (i.d. 4 mm) and included an in-bed thermowell and fused silica catalyst bed support. The catalyst particles (average size 0.17 mm) were placed on the support and held in place with glass wool. The reactor was placed in a cylindrical furnace, and the reactor temperature was controlled by a linear temperature-programmable controller. Rapid cooling of the reactor was achieved by lowering the furnace from the reactor.

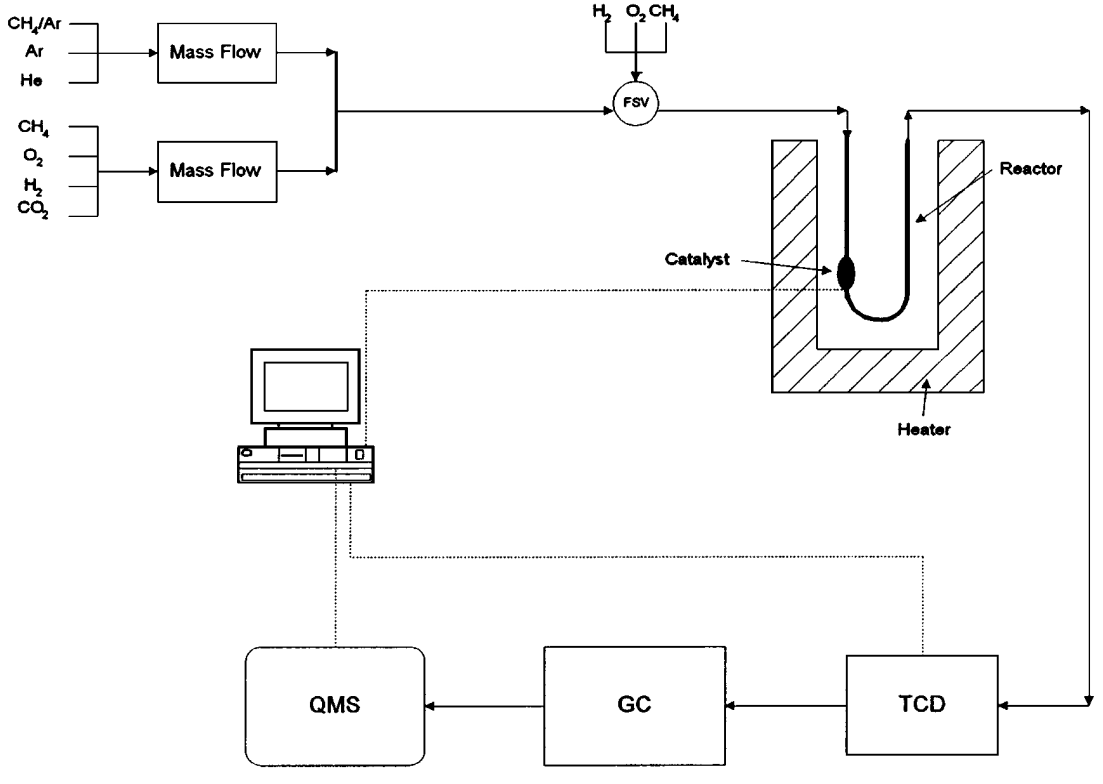

FIG. 1. Schematic of the experimental apparatus used in the present study. FSV, flow selector valve; TCD, thermal conductivity detector; GC, gas chromatograph; QMS, quadrupole mass spectrometer.

Product analysis was achieved in a variety of ways, depending on the type of experiment being performed. Hydrogen consumption during catalyst reduction was determined using a thermal conductivity detector (TCD). In this case the reactor feed gas was passed through the reference side of the TCD prior to entering the reactor (not shown in Fig. 1), while the reactor effluent was passed through the sample side of the same TCD. A Spectramass DAQ100/DXM quadrupole mass spectrometer (QMS) was used to continuously monitor the reaction products and a Varian 3400CX gas chromatograh (GC), equipped with a 10 loop sampling valve, was used to calibrate the QMS.

3. *Catalyst Characterization*

For the series A catalysts, temperature-programmed reduction (TPR) profiles were recorded by placing 0.5 g of the calcined catalyst in the reactor and increasing the temperature from 30 to 450°C at a ramp rate of 10°C/min while flowing 60 mL/min of a 20% H_2/80% Ar feed gas mixture. During the TPR measurement, the effluent gas was passed through a dry ice trap prior to entering the sample side of the TCD. The TCD response, which was proportional to the H_2 consumption, was recorded by data acquisition software. The H_2 consumption profile was integrated and calibrated against the H_2 consumption of a CuO (99.9%) standard during TPR. Hence, the degree of reduction of the calcined catalysts could be calculated (18).

Co dispersions were measured by a H_2 desorption method. Following TPR, the catalyst was cooled to 30°C in 20 mL/min of H_2, and then purged with 15 mL/min of Ar at 30°C for 30 min. The catalyst was then heated to 450°C within 3 min in 15 mL/min of Ar, and the H_2 desorption was monitored with the TCD. The H_2 desorption profile was calibrated against 0.1 mL pulses of H_2 under the same flow conditions. The catalyst was then purged for 15 min at 400°C in 15 mL/min of He. Subsequently, another measurement of the extent of catalyst reduction was performed by injecting pulses of O_2 (1 mL) into the He stream and monitoring the effluent with the TCD until no further O_2 uptake was observed. Assuming that during this process all the reduced Co was re-oxidized to Co_3O_4 at 400°C, the degree of reduction of the catalyst could be calculated.

For nominal Co loadings above 5 wt%, powder X-ray diffraction (XRD) patterns of both the calcined and reduced catalysts were recorded with a Siemens D5000 powder diffractometer. The size of both the Co_3O_4 and Co crystallites were estimated from Scherrer's peak broadening equation. For the case where XRD of the reduced catalysts was not performed, the Co_3O_4 particle size was converted to the corresponding Co metal particle size and hence dispersion using the equation $d_{Co} = 0.75 d_{Co_3O_4}$, which is based on a comparison of the molar volumes of Co and Co_3O_4 (19).

Characterization of the series C catalysts followed similar procedures and has been reported previously (17).

4. *Methane Decomposition*

Decomposition of CH_4 on the supported Co catalysts was performed in the same quartz, fixed-bed microreactor, with the same amount of catalyst as was used for the TPR and H_2 desorption measurements. Following TPR, the reactor and catalyst were purged with 48 mL/min of Ar at 450°C. Once the temperature and flow had reached steady-state, the reduced catalyst was exposed to a 5% CH_4/95% Ar gas mixture at a flowrate of 54 mL/min for periods of 2–7 min. During CH_4 decomposition, the reactor effluent was monitored continuously using the QMS.

RESULTS AND DISCUSSION

1. *Catalyst Characterization*

Table 1 summarizes the catalyst characterization data for the series A catalysts in which the nominal metal loading was varied from 2 to 12 wt% Co on SiO_2. By decreasing the nominal metal loading, the degree of reduction based on the O_2 uptake measurement decreased from 85 to 42%.

TABLE 1

Properties of Co Catalysts Used in Present Study

Series	Catalyst	Co loading (wt%)	Extent of reduction by		Co dispersion measured by	
			TPR in H_2 (mol%)	O_2 uptake (mol%)	H_2 desorption reduced catalyst (%)	XRD of Co_3O_4 calcined catalyst (%)
A	$Co–SiO_2$	12	91	85	5.6	10.0
A	$Co–SiO_2$	5	84	76	5.1	11.0
A	$Co–SiO_2$	2	—	42	5.3	—
C	$Co–SiO_2$	10	—	83	8.4	11.4
C	$K\text{-}Co–SiO_2$	10	—	84	5.2	—
C	$Co–Al_2O_3$	10	—	77	4.7	8.5
C	$K\text{-}Co–Al_2O_3$	10	—	67	4.0	—

The degree of reduction as calculated from the TPR measurement was in reasonable agreement with the O_2 uptake measurement on the reduced catalyst, and followed the same trend of decreased extent of reduction with decreased metal loading. Previous studies have reported somewhat lower levels of reduction for Co catalysts than those reported here (16, 18, 20). The higher values obtained in the present study are most likely due to the longer drying time and shorter calcination times used in the preparation of the catalysts. Generally, a low degree of reduction has been interpreted as evidence for the presence of cobalt silicates or a strong metal support interaction (SMSI) that results in cobalt species that are difficult to reduce (16, 18, 20).

The Co dispersions, reported as a percent of reduced Co and measured by H_2 desorption, did not show any strong dependence on metal loading. Of more significance, however, was the observation that the Co dispersions estimated by XRD line broadening were approximately twice the value measured by H_2 desorption. Similar differences were obtained for the series B catalysts, as shown in Table 2. Previous studies have shown that metal dispersions measured by XRD line broadening and H_2 chemisorption agree within approximately 30% (18, 20). Since our own repeat analyses showed the experimental error for each method to be better than $\pm 10\%$, and since the dispersions measured by H_2 desorption on the series C catalysts have been confirmed by XPS analysis (17), we conclude that the differences in dispersions estimated by XRD and chemisorption as shown in Tables 1 and 2 are significant.

The data of Tables 1 and 2 suggest that not all of the Co detected by XRD was exposed to H_2 in the chemisorption measurement. We interpret this observation as evidence for a metal support interaction (MSI) that involves migration of the SiO_2 support onto the reduced Co (21). A comparison of the difference between the XRD and chemisorption measurements for the 12 and 5 wt% Co catalysts (Table 1), suggests that this decoration of Co by SiO_2 became more significant as the metal loading decreased. Although SiO_2 is generally regarded as an inert support with weak MSI (22), previous studies have shown the importance of MSI with Co, including the effect of incomplete metal reduction (16, 18, 20) and alloy formation (23). Note that the presence of cobalt silicates or other unreduced Co species, as deduced from the incomplete cobalt reduction, cannot explain the difference in metal dispersions obtained by XRD and H_2 chemisorption.

TABLE 2

Comparison of Co Dispersion Measurements on 5% Co–SiO_2 Catalyst

Series	Extent of reduction (H_2 TPR) (mol%)	Co dispersion estimated from: H_2 desorption reduced catalyst (%)	XRD of Co reduced catalyst (%)	XRD of Co_3O_4 calcined catalyst (%)
B	75	4.9	7.3	8.5
B	82	4.3	7.3	9.2

The Co dispersion data estimated from XRD line broadening of Co_3O_4 and the relative molar volumes of Co_3O_4 and Co (19) were also compared to Co dispersions estimated from XRD line broadening of the reduced metal catalysts. Table 2 shows data for two series B catalysts that had different calcination treatments, both with a nominal 5% Co loading. The Co dispersions were measured by XRD line broadening and H_2 desorption of the reduced catalyst (Co), and by XRD line broadening of the calcined catalyst (Co_3O_4). As before, the Co dispersions estimated by XRD line broadening were greater than the values estimated by H_2 desorption. The Co dispersions estimated by line broadening of the reduced catalyst were lower but in reasonable agreement with the values estimated by line broadening of the Co_3O_4.

A report on the characterization of the C series catalysts was published previously (17), and Table 1 summarizes the degree of reduction and metal dispersion obtained for these catalysts.

2. *Decomposition of CH_4*

The QMS was used to monitor the reactor effluent stream during CH_4 decomposition. Figure 2 shows a typical profile of the turnover frequency (TOF) of consumption of CH_4 and generation of H_2, during a 2 min flow of 5% CH_4/95% Ar gas mixture at 450°C using the A series 12% Co–SiO_2 catalyst. The CH_4 consumption profile showed a short period of high reaction rate followed by a longer period of lower reaction rate. However, the rate of CH_4 consumption did not decrease to zero during the 2 min reaction period. By numerical integration of the CH_4 consumption and H_2 production molar rate profiles, the cumulative CH_4 consumption and H_2 generation were calculated as a function of the reaction time. Hence the cumulative CH_4 consumption per mole of surface Co on the reduced catalyst (the CH_4/Co ratio taken as a measure of the metal coverage) and the average value of x for the CH_x surface species could be calculated and are presented in Fig. 3.

A decrease in the slope of the cumulative CH_4 consumption curve is indicative of a decrease in the CH_4 consumption rate. As shown in Fig. 3, the slope decreased initially and then remained constant after approximately 1 min, corresponding to at least a monolayer coverage of the Co by CH_x (11). The data of Fig. 3 also show that the H content of the carbonaceous deposit decreased as the reaction time increased. Similar trends of decreasing x in CH_x surface species with increasing reaction time have been reported previously (1).

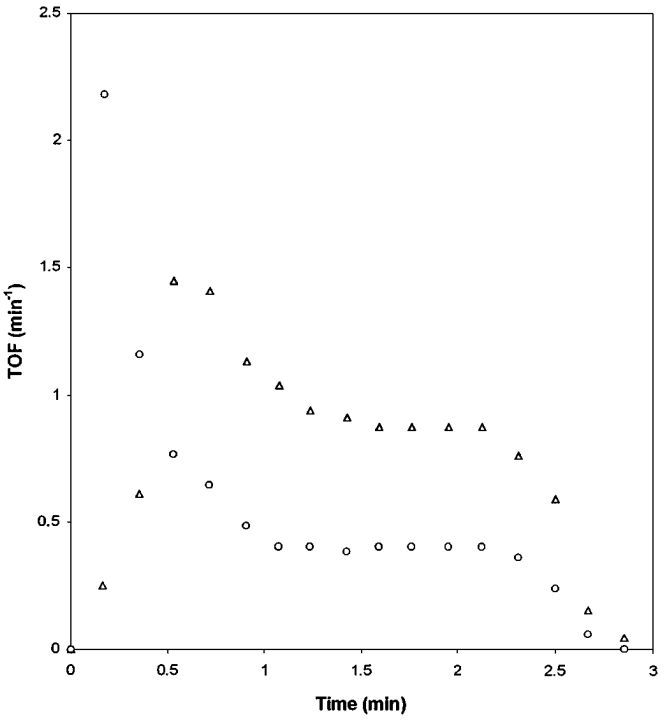

FIG. 2. Rate of CH_4 consumption (○) and H_2 production (△) per mole of surface Co during 2 min flow of 5% CH_4/95% Ar gas mixture at 54 mL/min at 450°C over the 12% Co–SiO_2 series A catalyst.

3. *Kinetics of CH_4 Decomposition*

The data of Fig. 2 clearly show that CH_4 consumption continued well beyond a nominal monolayer coverage of the metal sites. In addition, the data show that the species on the surface continued to lose hydrogen as time proceeded. To quantify these observations, a kinetic model of CH_4 decomposition was developed on the basis of published experimental and computational studies relevant to CH_4 decomposition.

Previous studies, reviewed recently by Guczi *et al.* (4), have shown that CH_4 interacts with metal surfaces to produce H_2 and some form of carbon species on the surface (1, 3, 17, 24, 25). Since the activation energy for the decomposition of gas phase CH_4 ($CH_{4(g)} + 2S \rightarrow CH_3S + HS$) is less than that of adsorbed CH_4 ($CH_4S + S \rightarrow CH_3S + HS$) over group VIII metal catalysts (26), it is reasonable to assume that the first step of the CH_4 decomposition reaction can be written according to reaction [1]. Furthermore, estimates of the activation energies for the subsequent dehydrogenation of CH_3S to CH_xS ($x = 2, 1, 0$) are 40–60 kJ/mol larger than those for the initial adsorption step (26). Hence it is reasonable to assume that subsequent dehydrogenation of surface CH_3 species generates H_2 and various carbon fragments CH_x ($x = 2, 1, 0$). Few studies on the structure of the carbonaceous fragments are available, although on Ru, vinylidene and methylidyne species have been identified (9, 28). Detection of small amounts of C_2H_6 and H_2 during the decomposition of CH_4 on supported Rh catalysts has been taken as evidence for the presence of surface CH_3 species (14, 28), the combination of which would yield C_2H_6. On the basis of these observations, but neglecting the combination reaction of surface carbon species because in the present work production of higher hydrocarbons (including C_2H_6) during the decomposition step was negligible, one can approximate the surface reactions according to the following sequence of steps:

$$CH_{4(g)} + 2S \rightarrow CH_3S + HS, \quad [1]$$

$$CH_3S + S \rightarrow CH_2S + HS, \quad [2]$$

$$CH_2S + S \rightarrow CHS + HS, \quad [3]$$

$$CHS + S \rightarrow CS + HS, \quad [4]$$

$$2HS \rightarrow H_2 + 2S, \quad [5]$$

where XS refers to an adsorbed surface species and S is the active metal site.

However, these steps imply that the rate of CH_4 decomposition will decrease with time due to the occupation of vacant sites and finally cease upon complete coverage of the metal sites by the carbonaceous species. Since experimental

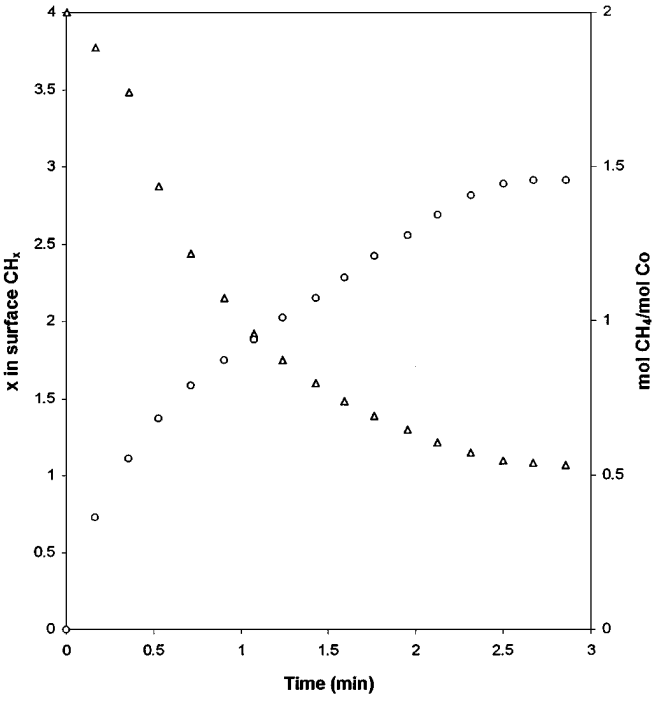

FIG. 3. Cumulative moles of CH_4 consumed per mole of surface Co (○) and the value of x in the CH_x surface species (△) during 2 min flow of 5% CH_4/95% Ar gas mixture at 54 mL/min at 450°C over the 12% Co–SiO_2 series A catalyst.

observations have shown that the supported metal catalysts activate more CH_4 than that corresponding to monolayer coverage (11, 17, 28, 29), migration or spillover of the carbon species from the metal site to the support was included in the kinetic model. Infrared studies of Cu–SiO_2 catalysts (15) have shown that CH_3 species generated from the decomposition of CH_3I on Cu, migrate onto the SiO_2 support where they interact with hydroxyl groups. Including the migration of all CH_xS ($x = 1, 2, 3$) surface species together with the dehydrogenation reactions would require an additional eight equations to describe the reaction mechanism. Because the present work is concerned primarily with CH_4 decomposition kinetics, the reaction mechanism was simplified further to reduce the number of rate constants in the kinetic model. Semiempirical calculations (25) indicate that highly hydrogenated CH_x fragments such as CH_3 are more mobile than, for example, CH_2 or CH, due to the weaker metal–adsorbate interaction of the CH_3 species. Consequently, migration from the metal site to the support site was assumed to be dominated by adsorbed CH_3 species. Furthermore, it was assumed that CH_3 adsorbed on both the metal and support is dehydrogenated to produce H_2 and a less hydrogenated carbon species. The simplified reaction mechanism follows:

$$CH_4 + 2S_1 \xrightarrow{k_1'} CH_3S_1 + HS_1, \quad [6]$$

$$CH_3S_1 + S_2 \xrightarrow{k_2'} CH_3S_2 + S_1, \quad [7]$$

$$2HS_1 \xrightarrow{k_3} H_2 + 2S_1, \quad [8]$$

$$CH_3S_1 \xrightarrow{k_4} CH_xS_1 + \frac{3-x}{2}H_2, \quad [9]$$

$$CH_3S_2 \xrightarrow{k_5} CH_xS_2 + \frac{3-x}{2}H_2, \quad [10]$$

where XS_1 refers to species X adsorbed on a metal site S_1 and XS_2 refers to species X adsorbed on the support site S_2.

Assuming that the coverage of support sites is relatively constant during CH_4 decomposition and the change in CH_4 concentration in the gas phase is negligible, one can write:

$$k_1 = k_1' P_{CH_4},$$
$$k_2 = k_2' \theta_{S_2}, \quad [11]$$

and the rate of change of coverage of different surface species follows directly from Eqs. [6]–[10]:

$$\frac{d\theta_{S_1}}{dt} = -2k_1\theta_{S_1}^2 + k_2\theta_{CH_3S_1} + k_3\theta_{HS_1}^2, \quad [12]$$

$$\frac{d\theta_{CH_3S_1}}{dt} = k_1\theta_{S_1}^2 - k_2\theta_{CH_3S_1} - k_4\theta_{CH_3S_1}, \quad [13]$$

$$\frac{d\theta_{HS_1}}{dt} = k_1\theta_{S_1}^2 - 2k_3\theta_{HS_1}^2, \quad [14]$$

$$\frac{d\theta_{CH_xS_1}}{dt} = k_4\theta_{CH_3S_1}, \quad [15]$$

$$\frac{d\theta_{CH_xS_2}}{dt} = k_5\theta_{CH_3S_2}. \quad [16]$$

The set of first-order differential equations is subject to the initial condition

$$\text{at } t = 0, \quad \theta_{S_1} = 1, \quad \theta_{CH_3S_1} = \theta_{HS_1} = \theta_{CH_xS_1} = \theta_{CH_xS_2} = 0, \quad [17]$$

where θ_j is the fractional surface coverage by species j.

Using Eqs. [6] and [8]–[10] the cumulative moles of CH_4 consumed and H_2 produced is given by

$$n_{CH_4} = -\int_0^t (mc_0)k_1\theta_{S_1}^2\, dt, \quad [18]$$

$$n_{H_2} = \int_0^t (mc_0)\left\{k_3\theta_{HS_1}^2 + \frac{3-x}{2}[k_4\theta_{CH_3S_1} + k_5\theta_{CH_3S_2}]\right\} dt, \quad [19]$$

where mc_0 is the total number of moles of surface metal sites.

The reaction mechanism proposed herein represents the carbon surface species as CH_x. Experimental data have shown that the value of x changes with reaction time (see Figs. 2 and 6) and with exposure to high temperature. To avoid the complicated problem of describing the transformation kinetics for CH_x species and the change in x (28), only the CH_4 consumption Eq. [18] together with Eqs. [12]–[15] was used to estimate the rate constants k_1, k_2, k_3, and k_4.

The rate constants were estimated using a combined pattern search and steepest descent optimization algorithm, with an initial guess of the rate constants. Using a fourth order Runge–Kutta method the set of initial value first-order differential equations was solved and the cumulative CH_4 consumption per surface Co (n_{CH_4}/mc_0) as a function of time was calculated. Using the sum of squares of the difference between the actual and calculated CH_4 consumption profiles as an objective function, the optimization routine improved the estimate of the rate constants until the minimum of the objective function corresponding to the optimum rate constants k_1, k_2, k_3, and k_4, was obtained.

Figure 4 is a typical comparison of the actual and calculated cumulative CH_4 consumption per surface Co molar ratio, as a function of time during CH_4 decomposition on the series A 12% Co–SiO_2 catalyst at 450°C for a 2 min reaction period. The estimated rate constants and

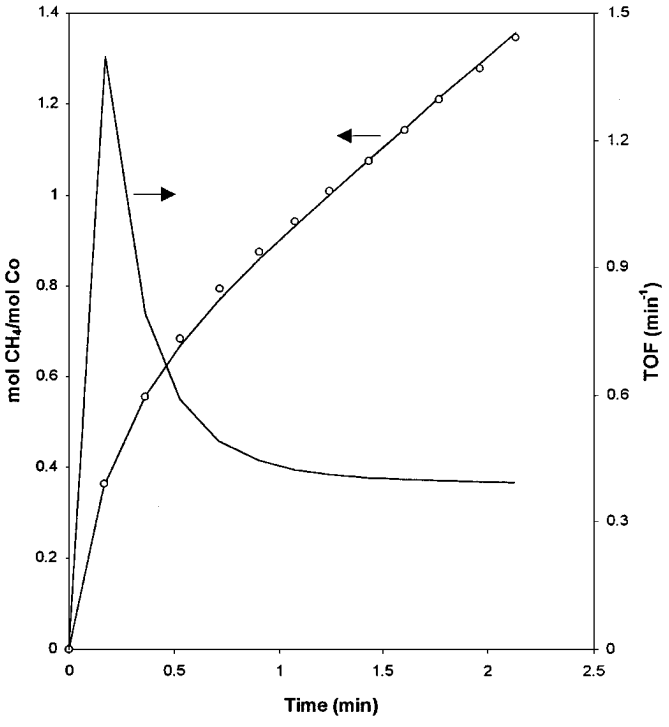

FIG. 4. Cumulative moles of CH_4 consumed per mole of surface Co (○) measured during 2 min flow of 5% CH_4/95% Ar gas mixture at 54 mL/min at 450°C over the 12% Co–SiO_2 series A catalyst, compared to model fit (—) (left axis). Calculated turnover frequency (TOF) profile of CH_4 consumption (right axis). Model parameter estimates given in the text.

their corresponding standard deviations were $k_1 = 3.9 \pm 0.2$ min^{-1}, $k_2 = 40.0 \pm 12.0$ min^{-1}, $k_3 = 0.5 \pm 0.1$ min^{-1}, and $k_4 = 1.1 \pm 0.3$ min^{-1}, and the agreement between the measured and calculated values was excellent ($R^2 = 99.9\%$). Note that without the migration step ($k_2 = 0$) the cumulative CH_4/Co molar ratio would asymptote to 1 and the decomposition rate would asymptote to zero (30). Clearly, the kinetic data are in accord with the proposed migration or spillover of CH_3 species from the Co to the support. Also shown in Fig. 4 is the calculated turnover frequency (TOF) for CH_4 consumption as a function of time. The TOF profile shows that after the initial fast reaction, the rate of CH_4 decomposition decreases asymptotically to a lower value but it does not drop to zero.

4. *Effect of Reaction Time*

In Fig. 5 the cumulative CH_4 consumption per surface Co molar ratio as a function of time for the series A 12% Co–SiO_2 catalyst is shown for a total reaction time of 7 min. These data were also well described by the kinetic model ($R^2 = 99.4\%$) with the estimated parameter values of $k_1 = 4.3 \pm 0.8$ min^{-1}, $k_2 = 54.3 \pm 12.3$ min^{-1}, $k_3 = 0.6 \pm 0.1$ min^{-1}, and $k_4 = 0.8 \pm 0.2$ min^{-1}. Taking account of the standard deviation of the estimates, these values were in good agreement with the estimates obtained from the 2 min reaction time experiment (Fig. 4). Figure 5 also shows the calculated TOF for CH_4 consumption as a function of reaction time. Similar to the 2 min reaction time (Fig. 4), the TOF of CH_4 consumption asymptotes to a non-zero constant value (about 0.4 min^{-1}).

Assuming that the carbon species on the surface can be represented as CH_x, the value of x as a function of reaction time, calculated from the measured CH_4 consumption and H_2 production data, is shown in Fig. 6. Increasing reaction time decreased the hydrogen content of the CH_x surface species. In previous reports with less than a monolayer coverage (1), x was reported to be close to 1.0. In addition, the presence of CH and C_2H_4 species on Ru catalysts has been detected spectroscopically after activation (28), and computational techniques (25) have shown that CH carbon species on a Pt catalyst can combine to form C_{2+} products more readily than CH_x species with $x > 1$. The data of Fig. 6 suggest that to obtain $x = 1$, a reaction time of about 2.5 min is required at the conditions of the present study. The continuous dehydrogenation of carbon species with reaction time is an indication of production of less active carbon species. This is in accordance with previous reports

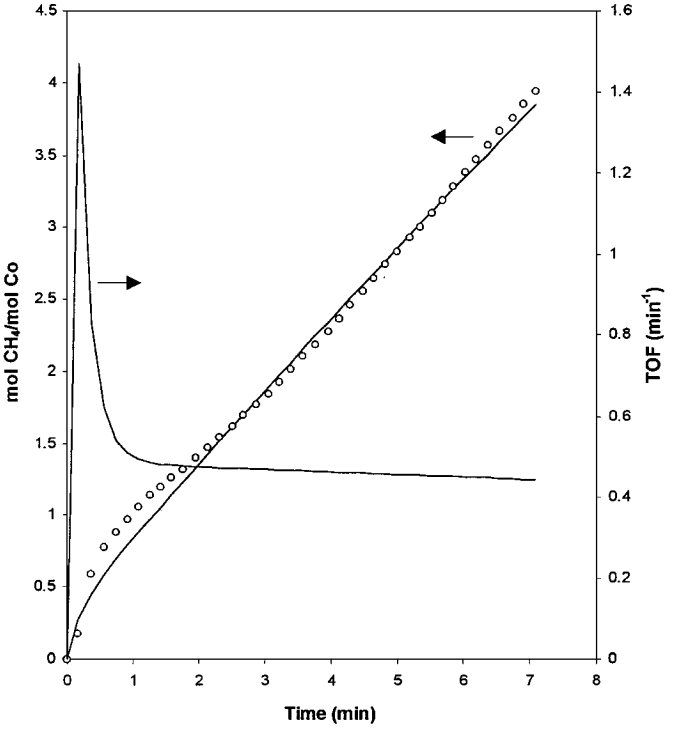

FIG. 5. Cumulative moles of CH_4 consumed per mole of surface Co (○) measured during 7 min flow of 5% CH_4/95% Ar gas mixture at 54 mL/min at 450°C over the 12% Co–SiO_2 series A catalyst, compared to model fit (—) (left axis). Calculated turnover frequency (TOF) profile of CH_4 consumption (right axis). Estimates of model parameter values given in the text.

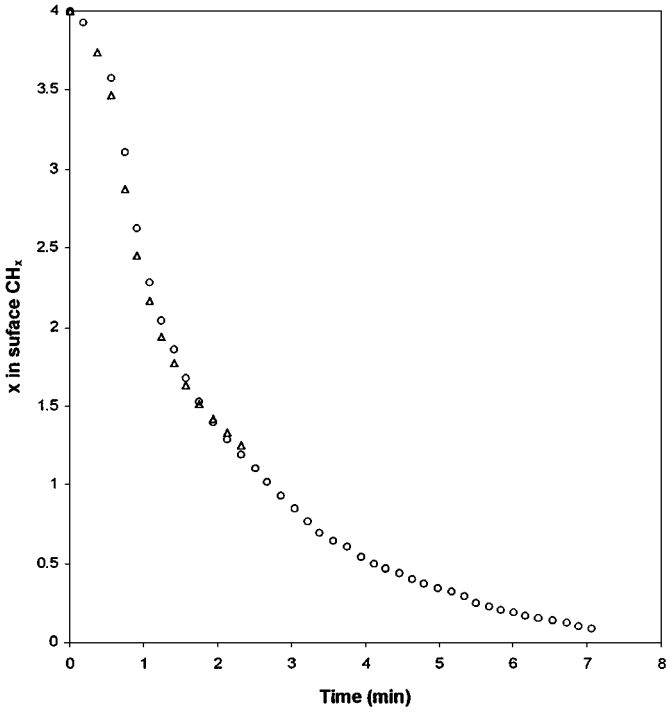

FIG. 6. Value of x in the CH_x surface species during 2 min (△) and 7 min (○) flow of 5% CH_4/95% Ar gas mixture at 54 mL/min at 450°C over the 12% Co–SiO_2 series A catalyst.

of transformation of more active carbon species to less active forms with increased reaction time (1).

5. *Effect of Catalyst Loading*

The A series Co–SiO_2 catalysts with 2, 5, and 12 wt% nominal Co were used to study the effect of catalyst metal loading on the CH_4 decomposition kinetics. Table 3 reflects the nominal metal coverage, reported as the moles of CH_4 reacted per mole of surface Co, and the estimated rate constants for CH_4 decomposition on the Co catalysts. The data of Table 1 showed that by decreasing the Co loading the extent of metal support interaction increased (i.e., lower extent of reduction and increased silica decoration of the reduced Co). Table 3 shows that an increased MSI not only increased the CH_4 decomposition activity (increased k_1), but also facilitated the migration of carbonaceous species from the metal to the support (increased k_2). Expectedly, the rate constant of the hydrogen combination reaction (k_3) was not influenced by the extent of the MSI. Although the electronic effect of supports on metal catalysts is generally considered a short-range effect (21), the increased MSI at lower loadings observed in the present study suggests that the overall electronic effect of the support on the metal becomes significant and results in an increase in k_1. In addition, as metal loading decreases the metal–support contact surface area is expected to increase, resulting in an increase in the rate of migration (increased k_2).

6. *Effect of Activation Temperature*

The series A 12% Co–SiO_2 catalyst was also used to study the effect of temperature on the CH_4 decomposition kinetics. The metal coverage, the value of x of the CH_x carbon species after a reaction time of 2 min, and the rate constants are reported in Table 4 for temperatures in the range 360–450°C. Increasing temperature increased the CH_4 conversion and the metal coverage (total moles of CH_4 reacted per mole of surface Co) but decreased the H content of the resulting surface species. The activation energies for initial activation of CH_4 on Co (k_1), migration of the CH_3 species to the support (k_2) and H_2 evolution (k_3) were estimated from the data of Table 4 as 56, 48, and 171 kJ/mol, respectively.

The activation energy for k_1 was in reasonable agreement with the value of 42 kJ/mol reported for the activation of CH_4 on Co–SiO_2 catalysts at less than a monolayer coverage (1). The apparent activation energy for the migration of CH_x species from Co to SiO_2 has not been reported. However, the activation energies for other surface diffusion phenomena (e.g., surface diffusion of CO on Ni and H spillover onto Al_2O_3) are of a similar magnitude (31, 32). The activation energy of hydrogen desorption from silica-supported Co catalysts has not been reported either. However, the activation energy distribution for hydrogen

TABLE 3

Effect of Catalyst Loading on the Reaction Rate Constants Estimated at 450°C and a 2 min Reaction Time with 5% CH_4 in Ar at 54 mL (STP)/min

Catalyst series A	CH_4 reacted mol CH_4/mol Co	Model parameters (min^{-1})				Std. error σ_e mol CH_4/mol Co	Regression coefficient R^2 (%)
		k_1	k_2	k_3	k_4		
12% Co–SiO_2	1.81	5	23	0.7	1.8	0.02	99.7
5% Co–SiO_2	2.01	117	153	0.5	12.0	0.06	98.5
2% Co–SiO_2	2.3	121	346	0.6	10.9	0.37	93.1

TABLE 4

Effect of Temperature on CH_4 Decomposition over 12% Co–SiO_2 Catalyst (Series A) Measured with a 2 min Reaction Time and 5% CH_4 in Ar at 54 mL (STP)/min

Temperature (°C)	Total CH_4 reacted: Ratio mol CH_4/mol Co	Total CH_4 reacted: Conv. (%)	x of CH_x	Model parameters (min^{-1}): k_1	k_2	k_3	k_4	σ_e mol CH_4/mol Co	R^2 (%)
360	0.5	7.2	2.1	1.4	5.9	0.01	0.87	0.01	99.9
390	0.6	9.8	1.4	2.0	5.1	0.24	1.13	0.03	99.2
450	1.3	20.8	0.9	5	16.8	0.56	1.24	0.01	99.7

desorption from silica-supported Ni catalysts has been reported to be in the range 35–135 kJ/mol, depending on the preparation method, metal loading, and surface coverage (33).

7. *Effect of Support and K Promoter on the Activation of CH_4*

Results of CH_4 activation on the C series 10% Co catalysts supported on SiO_2 and Al_2O_3, with and without 1 wt% K promoter (17) were also analyzed by the kinetic model. The experimental results and estimated rate constants are summarized in Table 5. Al_2O_3-supported Co catalysts showed a higher activity than SiO_2-supported catalysts (11, 17), and this observation is reflected in the higher value of k_1 estimated for the C series 10% Co–Al_2O_3 catalyst compared to the C series 10% Co–SiO_2 catalyst. Previously it was suggested that the differences in total CH_4 decomposition obtained with the different supports may be due to differences in the rate of migration of the carbonaceous deposit from the metal to the support (11). The kinetic analysis shows, however, that the rate of CH_4 decomposition (k_1) was more important, being much greater on the Al_2O_3-supported catalyst than the SiO_2-supported catalyst. Although differences in the estimated values of k_2 on the two supports are shown in Table 5, the parameter estimates were based on a 1 min activation time so that the effect of migration did not dominate the kinetic analysis. Hence, the estimated values of the parameters k_2, k_3, and k_4 have significant errors associated with them and definitive conclusions regarding the differences in the values of these parameters between the two supports were not possible.

The rate of migration (k_2) on the Al_2O_3- and SiO_2-supported catalysts increased significantly with addition of K promoter. The increase in k_2 may be due to the electron donor capability of the K promoter. The semiempirical calculations referred to previously (25) show that increased d orbital filling decreases the adsorption energy of the CH_3 species to the metal. Hence, addition of K would be expected to weaken the Co–CH_3 bond and thereby increase the rate of migration or spillover to the support site, in agreement with the kinetic model parameters.

CONCLUSIONS

The initial high rate of CH_4 decomposition on supported Co catalysts at 450°C and 101 kPa, decreased rapidly but continued despite a nominal coverage of the surface Co by CH_x that was >1. The kinetic model developed to describe this observation assumed decomposition of gas phase CH_4 on a Co site, followed by migration of the resulting CH_3 surface species from the Co to the support. Hence, the effects of reaction temperature, catalyst metal loading, support, and promoter could be interpreted in terms of the changes in the magnitudes of the decomposition and surface migration rate constants.

TABLE 5

Effect of Support and K Promoter on CH_4 Decomposition at 450°C and a Reaction Time of 1 min

Catalyst series C	Total CH_4 reacted: Ratio mol CH_4/mol Co	Total CH_4 reacted: Conv. (%)	Model parameters (min^{-1}): k_1	k_2	k_3	k_4	σ_c mol CH_4/mol Co	R^2 (%)
10% Co–SiO_2	1.15	37	5.8	18.6	74.1	11.0	0.05	98.5
K–10% Co–SiO_2	1.33	27	18.5	54.5	30.2	21.5	0.17	98.2
10% Co–Al_2O_3	1.92	32	17.7	11.5	57.4	5.6	0.08	99.1
K–10% Co–Al_2O_3	2.40	31	19.3	41.9	121.5	8.9	0.21	99.1

ACKNOWLEDGMENTS

Funding for the present study from the Natural Sciences and Engineering Research Council of Canada is gratefully acknowledged.

REFERENCES

1. Koerts, T., Deelen, M. J. A. G., and van Santen, R. A., *J. Catal.* **138**, 101 (1992).
2. Belgued, M., Amariglio, H., Pareja, P., Amariglio, A., and Saint-Just, J., *Catal. Today* **13**, 437 (1992).
3. Belgued, M., Amariglio, A., Lefort, A., Pareja, P., and Amariglio, H., *J. Catal.* **161**, 282 (1996).
4. Guczi, L., van Santen, R. A., and Sarma, K. V., *Catal. Rev.-Sci. Eng.* **38**(2), 249 (1996).
5. Fox, J. M., III, *Catal. Rev.-Sci. Eng.* **35**(2), 169 (1993).
6. Pitchai, R., and Klier, K., *Catal. Rev.-Sci. Eng.* **28**(1), 13 (1986).
7. Lunsford, J. H., *Angew. Chem., Int. Ed. Engl.* **34**, 970 (1995).
8. Poirier, M. G., Sanger, A. R., and Smith, K. J., *Can. J. Chem. Eng.* **69**, 1027 (1991).
9. Koranne, M. M., and Goodman, D. W., *Catal. Lett.* **30**, 219 (1995).
10. Carstens, J. N., and Bell, A. T., *J. Catal.* **161**, 423 (1996).
11. Boskovic, G., and Smith, K. J., *Catal. Today* **37**(1), 25 (1997).
12. Solymosi, F., Erdöhelyi, A., Cserényi, J., and Felvégi, A., *J. Catal.* **147**, 272 (1994).
13. Ferreira-Aparicio, P., Rodriguez-Ramos, I., and Guerrero-Ruiz, A., *Appl. Catal.* **148**, 343 (1997).
14. Erdöhelyi, A., Cserényi, J., and Solymosi, F., *J. Catal.* **141**, 287 (1993).
15. Driesen, M. D., and Grassian, V. H., *J. Catal.* **161**, 810 (1996).
16. Coulter, K. E., and Sault, A. G., *J. Catal.* **154**, 56 (1995).
17. Boskovic, G., Soltan Mohammad Zadeh, J., and Smith, K. J., *Catal. Lett.* **39**, 163 (1996).
18. Rosynek, M. P., and Polansky, C. A., *Appl. Catal.* **73**, 97 (1991).
19. Schanke, F., Vada, S., Blekkan, E. A., Hilmen, A. M., Huff, A., and Holmen, A., *J. Catal.* **156**, 85 (1995).
20. Reuel, R., and Bartholomew, C. H., *J. Catal.* **85**, 63 (1984).
21. Raupp, A. G., Stevenson, S. A., Dumesic, J. A., Tauster, S. J., and Baker, R. T. K., *in* "Metal Support Interactions in Catalysis, Sintering and Redispersion" (S. A. Stevenson, J. A. Dumeisc, R. T. K. Baker, and E. Ruckenstein, Eds.), Chap. 7, pp. 76–111. Van Nostrand Reinhold, New York, 1987.
22. Yoshitake, H., and Iwasawa, Y., *J. Phys. Chem.* **96**, 1329 (1992).
23. Potoczna-Petru, D., and Kepinski, L., *J. Mater. Sci.* **28**, 3501 (1993).
24. Solymosi, F., Erdöhelyi, A., and Cserényi, J., *Catal. Lett.* **16**, 399 (1992).
25. Koerts, T., and van Santen, R. A., *J. Mol. Catal.* **70**, 119 (1991).
26. Shustorovich, E., and Bell, A. T., *Surf. Sci.* **248**, 359 (1991).
27. Solymosi, F., and Cserényi, J., *Catal. Today* **21**, 561 (1994).
28. Lenz-Solomun, P., We, M.-C., and Goodman, D. W., *Catal. Lett.* **25**, 75 (1994).
29. Tsipouriari, V. A., Efstathiou, A. M., and Verykios, X. E., *J. Catal.* **161**, 31 (1996).
30. Kristyan, S., *Can. J. Chem. Eng.* **75**, 229 (1997).
31. Conner, W. C., Pajonk, G. M., and Teichner, S. J., *Adv. Catal.* **34**, 1 (1986).
32. Roop, B., Costello, S. A., Mullins, D. R., and White, J. M., *J. Chem. Phys.* **86**, 3003 (1987).
33. Arai, M., Nishiyama, Y., and Hashimoto, K., *Appl. Surf. Sci.* **89**(1), 11 (1995).